

A new Singular/Hypersingular MLPG (LBIE) method for 2D elastostatics

E. J. Sellountos¹, V. Vavourakis² and D. Polyzos³

Abstract: A new meshless local Petrov-Galerkin (MLPG) type method based on local boundary integral equation (LBIE) considerations is proposed for the solution of elastostatic problems. It is called singular/hypersingular MLPG (LBIE) method since the representation of the displacement field at the internal points of the considered structure is accomplished with the aid of the displacement local boundary integral equation, while for the boundary nodes both the displacement and the corresponding traction local boundary integral equations are employed. Nodal points spread over the analyzed domain are considered and the moving least squares (MLS) interpolation scheme for the approximation of the interior and boundary variables is employed. The essential boundary conditions are satisfied via the free terms of the singular and hypersingular LBIEs, respectively. This means that, for any distribution of nodal points, displacements and tractions can be treated as independent variables, avoiding thus derivatives of the MLS shape functions. On the local boundaries of the hypersingular LBIEs, tractions are avoided with the aid of an auxiliary local integral equation explicitly derived in the present work. Strongly singular and hypersingular integrals are evaluated directly and with high accuracy by means of advanced integration techniques. Two representative numerical examples that demonstrate the achieved accuracy of the proposed singular/hypersingular MLPG (LBIE) method are provided.

keyword: meshless methods, Meshless Local Petrov-Galerkin (MLPG) method, Local Boundary Integral Equation (LBIE) method, elasticity.

1 Introduction

The Boundary Element Method (BEM) is a well known and powerful numerical tool successfully used the last decades for the solution of both static and dynamic elastic problems [Beskos (1987); Beskos (1997); Agnatiaris and Polyzos (2003)]. However, problems associated with the unsymmetric and full-populated matrices of the final systems of linear equations taken by BEM confines the use of the method to problems dealing with structures where no a large number of elements is required for their numerical treatment. On the other hand, the requirement of using the fundamental solution of the differential equation that describes the problem of interest renders a BEM formulation questionable when non-linear, non-homogeneous and anisotropic elastic problems are considered.

The recently developed meshless method of Local Boundary Integral Equations (LBIE) proposed by [Zhu, Zhang, and Atluri (1998a)] seems to circumvent the aforementioned problems offering simultaneously the advantages of a meshless method where neither domain nor surface discretization is required. In this LBIE methodology a cloud of properly distributed nodal points covering the domain of interest as well as the surrounding global boundary is employed instead of any boundary or finite element discretization. All nodal points belong in regular sub-domains (e.g. circles for two-dimensional problems) centered at the corresponding collocation points. When non-linear elastic problems or elastic problems with body forces are considered, the displacement field at these sub-domains is described through the same surface integral equation used in the conventional static elastic BEM accompanied by volume integrals coming from the non-linear terms and/or the body forces appearing in the constitutive equations. The displacements at the local and global boundaries as well as in the interior of the sub-domains are usually approximated by a moving least square (MLS) scheme. Owing to regular shapes of the sub-domains, both surface

¹ Dept. of Mech. Engineering and Aeronautics; University of Patras (Greece)

² Dept. of Mech. Engineering and Aeronautics; University of Patras (Greece)

³ Dept. of Mech. Engineering and Aeronautics; University of Patras (Greece), Institute of Chem. Engng. and High Temperature Process ICETH-FORTH (Rio Greece)

and volume integrals are easily evaluated. The local nature of the sub-domains leads to a final linear system of equations the coefficient matrix of which is sparse and not full populated as in the case of the conventional BEM. At the same time with the LBIE method, Atluri and Zhu proposed a new meshless method [Atluri and Zhu (1998)], called Meshless Local Petrov-Galerkin (MLPG) method, as an alternative to the Finite Element Method (FEM). Depending on the test functions used in the weak formulation of the MLPG method, Atluri and co-workers developed six different MLPG methodologies numbered from one to six [Atluri and Shen (2002a); Atluri and Shen (2002b); Atluri, Han, and Shen (2003)]. The MLPG4 method utilizes as test functions, the fundamental solution of the differential equation (or part of the differential equation) of the problem, resulting thus to a MLPG approach that is equivalent to the LBIE method. Adopting this nomenclature, in the present work the LBIE method will be called from now and further MLPG (LBIE) method.

After the pioneering paper of [Zhu, Zhang, and Atluri (1998a)], several works on the MLPG (LBIE) method have been appeared in the literature. The most representative are those of [Zhu, Zhang, and Atluri (1998a); Zhu, Zhang, and Atluri (1998b); Zhu, Zhang, and Atluri (1999); Qian, Han, and Atluri (2004)], for linear and non-linear acoustic and potential problems, the works of [Sladek, Sladek, and Atluri (2000a); Atluri, Sladek, Sladek, and Zhu (2000); Sladek, Sladek, and Keer (2000); Atluri, Han, and Shen (2003); Han and Atluri (2004)] dealing with non-homogeneous and linear elastic problems, the works of [Long and Zhang (2002); Sladek, Sladek, and Mang (2002a); Sladek, Sladek, and Mang (2002b); Sladek, Sladek, and Mang (2003)] for plates, the papers of [Sladek, Sladek, and Atluri (2001)] and [Sladek, Sladek, Krivacek, and Zhang (2003)] concerning thermoelastic and transient heat conduction problems, respectively, and the works of [Sladek and Sladek (2003); Sladek, Sladek, and Bazant (2003)] for micropolar and non-local elastic problems. Details concerning the numerical implementation of a LBIE, integration techniques and the representation of field variables through meshless interpolation schemes can be found in the works of [Atluri and Zhu (1998); Atluri, Kim, and Cho (1999); Sladek, Sladek, and Keer (2000)]. Finally, a comprehensive presentation on the application of the LBIE method to different types of boundary value problems one can find in the review paper of [Sladek, Sladek,

and Atluri (2002)] and in the very recent book of [Atluri (2004)].

Very recently, [Sellountos and Polyzos (2003); Sellountos and Polyzos (2004a); Sellountos and Polyzos (2004b)] proposed a new MLPG (LBIE) method for solving static, quasi-static and transient linear elastic problems. The new elements of this method as it is compared to the corresponding ones proposed mainly by Atluri, Sladek brothers and co-workers are (i) it employs either the static or the frequency domain elastodynamic fundamental solution, (ii) on the global boundary displacements and tractions are treated as independent variables, avoiding thus derivatives of the MLS shape functions, (iii) it utilizes relatively uniform distribution of nodal points so that, in the global boundary, the MLS interpolation scheme to possess δ -property [Gosz and Liu (1996)] and the essential boundary conditions to be imposed directly on the fictitious nodal displacements and tractions, (iv) the surface and volume integrals are evaluated accurately with the aid of some practical and accurate techniques and (v) the strongly singular integrals are computed directly and with high accuracy by employing the expansion technique of [Guiggiani and Casalini (1987)]. Although accurate, the above methodology appears the problem of requiring a relatively uniform distribution of nodal points throughout the analyzed domain. In the present work a new version of the MLPG (LBIE) method of [Sellountos and Polyzos (2003)], valid for any distribution of points, is proposed. It is called singular/hypersingular MLPG (LBIE) method since the representation of the displacement field at the internal points of the considered structure is accomplished with the aid of the displacement local boundary integral equation, while for the boundary nodes both the displacement and the corresponding traction local boundary integral equations are employed. The essential displacement and traction boundary conditions of the problem are satisfied via the free terms of the singular and hypersingular local boundary equations, respectively. For any distribution of nodal points, displacements and tractions are treated as independent variables, avoiding thus derivatives of the MLS shape functions. On the local boundaries of the hypersingular local boundary equations, tractions are avoided with the aid of an auxiliary local integral equation explicitly derived in the framework of the present work. The hypersingular integrals are evaluated directly and with high accuracy by means of a direct integration technique proposed by [Guiggiani, Krishnasamy, Rudol-

phi, and Rizzo (1992); Guiggiani (1994)]. The paper is organized as follows: in the next section the displacement and traction local boundary integral equations are presented. The MLS interpolation scheme used for the representation of the unknown displacements and boundary tractions is demonstrated in section 3. In the forth section the numerical implementation of the proposed methodology is explained. Finally, in section 5 the accuracy of the singular/hypersingular MLPG (LBIE) method is demonstrated through two representative numerical examples.

2 Local Integral Equations

In this section the two local integral equations used for the formulation of the proposed here Singular/Hypersingular LBIE method are explicitly derived.

2.1 Displacement Local Boundary Integral Equations

Consider a two-dimensional linear elastic domain of volume Ω with a smooth boundary Γ . Neglecting body forces, the displacement field \mathbf{u} at any point \mathbf{x} satisfies the well-known Navier-Cauchy equation [Timoshenko and Goodier (1970)]

$$\mu \nabla^2 \mathbf{u}(\mathbf{x}) + (\lambda + \mu) \nabla \nabla \cdot \mathbf{u}(\mathbf{x}) = \mathbf{0} \quad (1)$$

where λ and μ are the Lamé constants and ∇ is the gradient operator. The boundary conditions are assumed to be

$$\begin{aligned} \mathbf{u}(\mathbf{x}) &= \bar{\mathbf{u}}(\mathbf{x}), \mathbf{x} \in \Gamma_u \\ \mathbf{t}(\mathbf{x}) &= \bar{\mathbf{t}}(\mathbf{x}), \mathbf{x} \in \Gamma_t \end{aligned} \quad (2)$$

with $\bar{\mathbf{u}}$, $\bar{\mathbf{t}}$ representing prescribed displacement and traction vectors, respectively, on the global boundary $\Gamma_u \cup \Gamma_t \equiv \Gamma$.

The integral representation of the above described problem is [Brebbia and Dominguez (1989)]

$$\begin{aligned} a \mathbf{u}(\mathbf{x}) + \int_S \tilde{\mathbf{t}}^*(\mathbf{x}, \mathbf{y}) \cdot \mathbf{u}(\mathbf{y}) dS_y = \\ \int_S \tilde{\mathbf{u}}^*(\mathbf{x}, \mathbf{y}) \cdot \mathbf{t}(\mathbf{y}) dS_y \end{aligned} \quad (3)$$

where $a = 1/2$ for boundary points \mathbf{x} and $a = 1$ for internal ones, \mathbf{u}^* , \mathbf{t}^* are the fundamental displacement and traction tensors, respectively, having the form [Brebbia

and Dominguez (1989)]

$$\tilde{\mathbf{u}}^*(\mathbf{x}, \mathbf{y}) = \frac{1}{2\pi\mu} [\Psi^* \tilde{\mathbf{I}} - X^* \hat{\mathbf{r}} \otimes \hat{\mathbf{r}}] \quad (4)$$

$$\begin{aligned} \tilde{\mathbf{t}}^*(\mathbf{x}, \mathbf{y}) = -\frac{1}{2\pi} \left\{ \left(\frac{X^*}{r} - \frac{d\Psi^*}{dr} \right) (\hat{\mathbf{r}} \cdot \hat{\mathbf{n}}) \tilde{\mathbf{I}} + \right. \\ \left. 2 \left(\frac{dX^*}{dr} - \frac{2X^*}{r} \right) (\hat{\mathbf{r}} \cdot \hat{\mathbf{n}}) \hat{\mathbf{r}} \otimes \hat{\mathbf{r}} + \left(\frac{X^*}{r} - \frac{d\Psi^*}{dr} \right) \hat{\mathbf{n}} \otimes \hat{\mathbf{r}} - \right. \\ \left. \left[\frac{2\nu}{1-2\nu} \left(\frac{d\Psi^*}{dr} - \frac{dX^*}{dr} - \frac{X^*}{r} \right) - \frac{2X^*}{r} \right] \hat{\mathbf{r}} \otimes \hat{\mathbf{n}} \right\} \end{aligned} \quad (5)$$

with

$$\begin{aligned} \Psi^* &= \frac{3-4\nu}{4(1-\nu)} \ln \frac{1}{r} \\ X^* &= -\frac{1}{4(1-\nu)} \end{aligned} \quad (6)$$

where ν is the Poisson ratio, $\hat{\mathbf{r}} = (\mathbf{x} - \mathbf{y}) / |\mathbf{x} - \mathbf{y}|$, $\hat{\mathbf{n}}$ is the outward unit normal vector to boundary Γ , $\tilde{\mathbf{I}}$ is the unit tensor and the symbol \otimes denotes dyadic product.

Since both \mathbf{u}^* and \mathbf{t}^* become singular only when \mathbf{y} approaches \mathbf{x} , it is easy to see one that the integral Eq.(3) can also be written in the form

$$\begin{aligned} a \mathbf{u}(\mathbf{x}) + \int_{\partial\Omega_x \cup \Gamma_x} \tilde{\mathbf{t}}^*(\mathbf{x}, \mathbf{y}) \cdot \mathbf{u}(\mathbf{y}) dS_y = \\ \int_{\partial\Omega_x \cup \Gamma_x} \tilde{\mathbf{u}}^*(\mathbf{x}, \mathbf{y}) \cdot \mathbf{t}(\mathbf{y}) dS_y \end{aligned} \quad (7)$$

where $\partial\Omega_x$ is the boundary of a small circle $\Omega_x \subset \Omega$, called support domain, centered at the field point \mathbf{x} and Γ_x is the part of Γ intersected by the subdomain Ω_x , as shown in Fig.1.

As it is explained in the work of [Atluri and Zhu (2000)], the integral Eq.(7) can be further simplified by eliminating the unknown traction vectors defined on the circular local boundaries $\partial\Omega_x$. This can be accomplished with the aid of a companion solution $\tilde{\mathbf{u}}^c$, as it is explained below. Consider a regular function of r satisfying the following boundary value problem:

$$\mathfrak{D}_y \tilde{\mathbf{u}}^c(\mathbf{x}, \mathbf{y}) = \mathbf{0}, \mathbf{y} \in \Omega_x \quad (8)$$

$$\mathfrak{D}_y \equiv \mu \nabla_y^2 + (\lambda + \mu) \nabla_y \nabla_y \cdot \quad (9)$$

$$\tilde{\mathbf{u}}^c(\mathbf{x}, \mathbf{y}) = \tilde{\mathbf{u}}^*(\mathbf{x}, \mathbf{y}), \mathbf{y} \in \partial\Omega_x \quad (10)$$

The solution of this problem is called companion solution [Atluri and Zhu (2000)] and has the form [Sellountos and Polyzos (2003)]

$$\tilde{\mathbf{u}}^c(\mathbf{x}, \mathbf{y}) = \frac{1}{2\pi\mu} [\Psi^c \tilde{\mathbf{I}} - X^c \hat{\mathbf{r}} \otimes \hat{\mathbf{r}}] \quad (11)$$

with

$$\begin{aligned} \Psi^c &= \frac{1}{4(1-\nu)} \left[\frac{5-4\nu}{2(3-4\nu)} \left(1 - \frac{r^2}{r_0^2} \right) + (4\nu - 3) \ln r_0 \right] \\ X^c &= -\frac{1}{4(1-\nu)} \frac{r^2}{r_0^2} \end{aligned} \quad (12)$$

where r_0 is the radius of the local circular subdomain Ω_x (see Fig.1).

Applying Betti's reciprocal identity for the fields \mathbf{u} and $\tilde{\mathbf{u}}^c$ one obtains

$$\int_{\Omega_x} [\mathcal{D}_y \tilde{\mathbf{u}}^c(\mathbf{x}, \mathbf{y}) \cdot \mathbf{u}(\mathbf{y}) - \tilde{\mathbf{u}}^c(\mathbf{x}, \mathbf{y}) \cdot \mathcal{D}_y \mathbf{u}(\mathbf{y})] dV_y = \int_{\partial\Omega_x \cup \Gamma_x} [\tilde{\mathbf{t}}^c(\mathbf{x}, \mathbf{y}) \cdot \mathbf{u}(\mathbf{y}) - \tilde{\mathbf{u}}^c(\mathbf{x}, \mathbf{y}) \cdot \mathbf{t}(\mathbf{y})] dS_y \quad (13)$$

Making use of Eq.(8) and taking into account that $\tilde{\mathbf{u}}^c$ satisfies the Navier-Cauchy Eq.(1), Eq.(13) is reduced to

$$\int_{\partial\Omega_x \cup \Gamma_x} \tilde{\mathbf{u}}^c(\mathbf{x}, \mathbf{y}) \cdot \mathbf{t}(\mathbf{y}) dS_y = \int_{\partial\Omega_x \cup \Gamma_x} \tilde{\mathbf{t}}^c(\mathbf{x}, \mathbf{y}) \cdot \mathbf{u}(\mathbf{y}) dS_y \quad (14)$$

On the other hand, it is easy to see one that Eq.(7) can be written as

$$\mathbf{a} \mathbf{u}(\mathbf{x}) + \int_{\partial\Omega_x \cup \Gamma_x} \tilde{\mathbf{t}}^*(\mathbf{x}, \mathbf{y}) \cdot \mathbf{u}(\mathbf{y}) dS_y = \int_{\partial\Omega_x \cup \Gamma_x} \tilde{\mathbf{u}}^c(\mathbf{x}, \mathbf{y}) \cdot \mathbf{t}(\mathbf{y}) dS_y + \int_{\partial\Omega_x \cup \Gamma_x} [\tilde{\mathbf{u}}^*(\mathbf{x}, \mathbf{y}) - \tilde{\mathbf{u}}^c(\mathbf{x}, \mathbf{y})] \cdot \mathbf{t}(\mathbf{y}) dS_y \quad (15)$$

In view of Eqs.(10) and (14), Eq.(15) leads to the following set of local integral equations:

$$\mathbf{u}(\mathbf{x}) + \int_{\partial\Omega_x} [\tilde{\mathbf{t}}^*(\mathbf{x}, \mathbf{y}) - \tilde{\mathbf{t}}^c(\mathbf{x}, \mathbf{y})] \cdot \mathbf{u}(\mathbf{x}) dS_y = \mathbf{0} \quad (16)$$

$$\mathbf{a} \mathbf{u}(\mathbf{x}) + \int_{\partial\Omega_x \cup \Gamma_x} [\tilde{\mathbf{t}}^*(\mathbf{x}, \mathbf{y}) - \tilde{\mathbf{t}}^c(\mathbf{x}, \mathbf{y})] \cdot \mathbf{u}(\mathbf{x}) dS_y = \int_{\Gamma_x} [\tilde{\mathbf{u}}^*(\mathbf{x}, \mathbf{y}) - \tilde{\mathbf{u}}^c(\mathbf{x}, \mathbf{y})] \cdot \mathbf{t}(\mathbf{x}) dS_y \quad (17)$$

where Eq.(16) represents the displacement local boundary integral equation of an internal point whose support domain does not intersect the global boundary Γ , while Eq.(17) is referred to a boundary or internal point that its circle $\partial\Omega_x$ intersects Γ .

2.2 Traction Local Boundary Integral Equations

The traction vector \mathbf{t} at a boundary point \mathbf{x} can be obtained by applying Hooke's law on Eq.(7) and taking the inner product with the unit vector $\hat{\mathbf{n}}_x$ being normal to the global boundary Γ at point \mathbf{x} , i.e.

$$\mathbf{a} \mathbf{t}(\mathbf{x}) + \int_{\partial\Omega_x \cup \Gamma_x} \tilde{\mathbf{p}}^*(\mathbf{x}, \mathbf{y}) \cdot \mathbf{u}(\mathbf{y}) dS_y = \int_{\partial\Omega_x \cup \Gamma_x} \tilde{\mathbf{v}}^*(\mathbf{x}, \mathbf{y}) \cdot \mathbf{t}(\mathbf{y}) dS_y \quad (18)$$

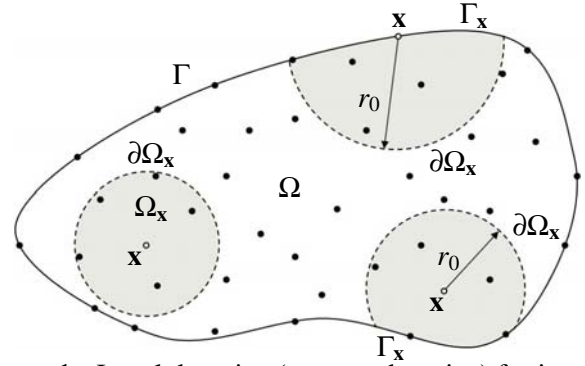


Figure 1 : Local domains (support domains) for internal and boundary nodes.

where the kernels $\tilde{\mathbf{v}}^*$ and $\tilde{\mathbf{p}}^*$ have the form [Polyzos, Tsinopoulos, and Beskos (1998); do Rego Silva (1994)]:

$$\tilde{\mathbf{v}}^*(\mathbf{x}, \mathbf{y}) = \frac{1}{2\pi} \left\{ \left(\frac{X^*}{r} - \frac{d\Psi^*}{dr} \right) [\hat{\mathbf{n}}_x \otimes \hat{\mathbf{r}} + (\hat{\mathbf{n}}_x \cdot \hat{\mathbf{r}}) \tilde{\mathbf{I}}] + 2 \left(\frac{dX^*}{dr} - \frac{2X^*}{r} \right) (\hat{\mathbf{n}}_x \cdot \hat{\mathbf{r}}) \hat{\mathbf{r}} \otimes \hat{\mathbf{r}} - \left[\frac{2\nu}{1-2\nu} \left(\frac{d\Psi^*}{dr} - \frac{dX^*}{dr} - \frac{X^*}{r} \right) - \frac{2X^*}{r} \right] \hat{\mathbf{r}} \otimes \hat{\mathbf{n}}_x \right\} \quad (19)$$

$$\tilde{\mathbf{p}}^*(\mathbf{x}, \mathbf{y}) = \frac{\mu}{2\pi} [\alpha_1(r) (\hat{\mathbf{n}}_y \cdot \hat{\mathbf{r}}) \hat{\mathbf{n}}_x \otimes \hat{\mathbf{r}} + \alpha_2(r) (\hat{\mathbf{n}}_y \cdot \hat{\mathbf{r}}) (\hat{\mathbf{n}}_x \cdot \hat{\mathbf{r}}) \tilde{\mathbf{I}} + \alpha_2(r) (\hat{\mathbf{n}}_y \cdot \hat{\mathbf{r}}) \hat{\mathbf{r}} \otimes \hat{\mathbf{n}}_x - \alpha_3(r) (\hat{\mathbf{n}}_y \cdot \hat{\mathbf{r}}) (\hat{\mathbf{n}}_x \cdot \hat{\mathbf{r}}) \hat{\mathbf{r}} \otimes \hat{\mathbf{r}} + \alpha_2(r) (\hat{\mathbf{n}}_y \cdot \hat{\mathbf{n}}_x) \hat{\mathbf{r}} \otimes \hat{\mathbf{r}} + \alpha_2(r) (\hat{\mathbf{n}}_x \cdot \hat{\mathbf{r}}) \hat{\mathbf{n}}_y \otimes \hat{\mathbf{r}} + \alpha_1(r) (\hat{\mathbf{n}}_x \cdot \hat{\mathbf{r}}) \hat{\mathbf{r}} \otimes \hat{\mathbf{n}}_y + \alpha_4(r) (\hat{\mathbf{n}}_y \cdot \hat{\mathbf{n}}_x) \tilde{\mathbf{I}} + \alpha_4(r) \hat{\mathbf{n}}_y \otimes \hat{\mathbf{n}}_x - \alpha_5(r) \hat{\mathbf{n}}_x \otimes \hat{\mathbf{n}}_y] \quad (20)$$

where

$$\begin{aligned} \alpha_1(r) &= \frac{4}{r} \frac{dX^*}{dr} - \frac{8X^*}{r} + \frac{4\nu}{1-2\nu} \left(\frac{d^2X^*}{dr^2} - \frac{d^2\Psi^*}{dr^2} + \frac{1}{r} \frac{d\Psi^*}{dr} - \frac{2X^*}{r^2} \right) \\ \alpha_2(r) &= -\frac{d^2\Psi^*}{dr^2} + \frac{1}{r} \frac{d\Psi^*}{dr} + \frac{3}{r} \frac{dX^*}{dr} - \frac{6X^*}{r^2} \\ \alpha_3(r) &= -4 \left(\frac{d^2X^*}{dr^2} - \frac{5}{r} \frac{dX^*}{dr} + \frac{8X^*}{r^2} \right) \\ \alpha_4(r) &= -\frac{2}{r} \frac{d\Psi^*}{dr} + \frac{2X^*}{r^2} \\ \alpha_5(r) &= -\frac{4X^*}{r^2} - \frac{8\nu}{1-2\nu} \left(\frac{1}{r} \frac{dX^*}{dr} - \frac{1}{r} \frac{d\Psi^*}{dr} + \frac{X^*}{r^2} \right) + \left(\frac{2\nu}{1-2\nu} \right)^2 \left(\frac{d^2\Psi^*}{dr^2} - \frac{d^2X^*}{dr^2} - \frac{2}{r} \frac{dX^*}{dr} + \frac{1}{r} \frac{d\Psi^*}{dr} \right) \end{aligned} \quad (21)$$

In order to get rid of the tractions defined on the local boundary $\partial\Omega_x$, the following auxiliary local integral equation, derived in Appendix, is exploited

$$\int_{\partial\Omega_x \cup \Gamma_x} \tilde{\mathbf{p}}^{\text{aux}}(\mathbf{x}, \mathbf{y}) \cdot \mathbf{u}(\mathbf{x}) dS_y = \int_{\partial\Omega_x \cup \Gamma_x} \tilde{\mathbf{v}}^{\text{aux}}(\mathbf{x}, \mathbf{y}) \cdot \mathbf{t}(\mathbf{x}) dS_y - \int_{\Omega_x} \tilde{\mathbf{b}}^{\text{aux}}(\mathbf{x}, \mathbf{y}) \cdot \mathbf{u}(\mathbf{y}) dV_y \quad (22)$$

where the kernels $\tilde{\mathbf{v}}^{\text{aux}}$, $\tilde{\mathbf{p}}^{\text{aux}}$ and $\tilde{\mathbf{b}}^{\text{aux}}$ are given in the Appendix.

Subtracting Eq.(22) from Eq.(18) one obtains

$$\begin{aligned} a \mathbf{t}(\mathbf{x}) + \int_{\partial\Omega_{\mathbf{x}} \cup \Gamma_{\mathbf{x}}} [\tilde{\mathbf{p}}^*(\mathbf{x}, \mathbf{y}) - \tilde{\mathbf{p}}^{\text{aux}}(\mathbf{x}, \mathbf{y})] \cdot \mathbf{u}(\mathbf{x}) dS_{\mathbf{y}} = \\ \int_{\partial\Omega_{\mathbf{x}} \cup \Gamma_{\mathbf{x}}} [\tilde{\mathbf{v}}^*(\mathbf{x}, \mathbf{y}) - \tilde{\mathbf{v}}^{\text{aux}}(\mathbf{x}, \mathbf{y})] \cdot \mathbf{t}(\mathbf{x}) dS_{\mathbf{y}} - \\ \int_{\Omega_{\mathbf{x}}} \tilde{\mathbf{b}}^{\text{aux}}(\mathbf{x}, \mathbf{y}) \cdot \mathbf{u}(\mathbf{y}) dV_{\mathbf{y}} \end{aligned} \quad (23)$$

Making use of the property of $\tilde{\mathbf{v}}^{\text{aux}}$ (see Appendix)

$$\tilde{\mathbf{v}}^{\text{aux}}(\mathbf{x}, \mathbf{y}) = \tilde{\mathbf{v}}^*(\mathbf{x}, \mathbf{y}), \quad \mathbf{y} \in \partial\Omega_{\mathbf{x}} \quad (24)$$

the hypersingular local boundary integral Eq.(23) is finally written as

$$\begin{aligned} a \mathbf{t}(\mathbf{x}) + \int_{\partial\Omega_{\mathbf{x}} \cup \Gamma_{\mathbf{x}}} [\tilde{\mathbf{p}}^*(\mathbf{x}, \mathbf{y}) - \tilde{\mathbf{p}}^{\text{aux}}(\mathbf{x}, \mathbf{y})] \cdot \mathbf{u}(\mathbf{x}) dS_{\mathbf{y}} = \\ \int_{\Gamma_{\mathbf{x}}} [\tilde{\mathbf{v}}^*(\mathbf{x}, \mathbf{y}) - \tilde{\mathbf{v}}^{\text{aux}}(\mathbf{x}, \mathbf{y})] \cdot \mathbf{t}(\mathbf{x}) dS_{\mathbf{y}} - \\ \int_{\Omega_{\mathbf{x}}} \tilde{\mathbf{b}}^{\text{aux}}(\mathbf{x}, \mathbf{y}) \cdot \mathbf{u}(\mathbf{y}) dV_{\mathbf{y}} \end{aligned} \quad (25)$$

3 MLS approximation of displacements and tractions

The Moving Least Squares (MLS) approximation is the most widely used interpolation scheme in the mesh-free numerical methods, appearing to date in the literature. Details on the subject can be found in the papers of [Lancaster and Salkauskas (1981); Krysl and Belytschko (1997); Atluri, Kim, and Cho (1999)]. In this section the MLS approximation is presented in brief.

Consider a set of properly distributed nodal points covering the boundary and the interior space of the analyzed domain Ω . At each point $\mathbf{x}^{(k)}$ corresponds a circular subdomain $\Omega_{(k)} \subset \Omega$ of radius $r_0^{(k)}$ called support domain of node $\mathbf{x}^{(k)}$, as shown in Fig.2. For any given internal or boundary point \mathbf{x} , the support subdomains $\Omega_{(j)}$ of the adjacent nodes $\mathbf{x}^{(j)}$, $j = 1, \dots, n$ that contain the point \mathbf{x} define a non-circular subdomain $\hat{\Omega}_{\mathbf{x}} = \Omega_{(1)} \cup \dots \cup \Omega_{(n)}$ called domain-of-definition of the MLS approximation field at \mathbf{x} . For any internal nodal point $\mathbf{x}^{(j)} \in \Omega_{(k)}$ each component $u_i(\mathbf{x})$, $i = 1, 2$ of the above function is approximated as

$$u_i(\mathbf{x}) = \mathbf{p}(\mathbf{x}) \cdot \mathbf{a}^{(i)}(\mathbf{x}) \quad (26)$$

with \mathbf{p} being a vector the m components of which form a complete basis of monomials of the spatial variables x_i and $\mathbf{a}^{(i)}$ is a coefficient vector. The m unknown coefficients of $\mathbf{a}^{(i)}$ are determined by minimizing the weighted discrete L_2 -norm

$$J_i = \sum_{j=1}^n w(\mathbf{x} - \mathbf{x}^{(j)}) \left[\mathbf{p}(\mathbf{x}^{(j)}) \cdot \mathbf{a}^{(i)}(\mathbf{x}) - \hat{u}_i(\mathbf{x}^{(j)}) \right]^2 \quad (27)$$

where $\hat{u}_i(\mathbf{x}^{(j)})$ is the unknown fictitious nodal displacement component at node $\mathbf{x}^{(j)}$ and $w(\mathbf{x} - \mathbf{x}^{(j)})$ is the Gaussian weighted function [Atluri and Zhu (2000)]. The minimization of J_i leads to the linear relation:

$$\tilde{\mathbf{A}}(\mathbf{x}, \mathbf{x}^{(j)}) \cdot \mathbf{a}^{(i)}(\mathbf{x}) = \tilde{\mathbf{B}}(\mathbf{x}, \mathbf{x}^{(j)}) \cdot \hat{\mathbf{u}}^{(i)} \quad (28)$$

where

$$\hat{\mathbf{u}}^{(i)} = [\hat{u}_i(\mathbf{x}^{(1)}) \quad \dots \quad \hat{u}_i(\mathbf{x}^{(n)})]^T \quad (29)$$

$$\tilde{\mathbf{A}}(\mathbf{x}, \mathbf{x}^{(j)}) = \sum_{l=1}^n w(\mathbf{x} - \mathbf{x}^{(l)}) \mathbf{p}(\mathbf{x}^{(l)}) \otimes \mathbf{p}(\mathbf{x}^{(l)}) \quad (30)$$

$$\tilde{\mathbf{B}}(\mathbf{x}, \mathbf{x}^{(j)}) = \left\{ \begin{array}{c} w(\mathbf{x} - \mathbf{x}^{(1)}) \mathbf{p}(\mathbf{x}^{(1)}) \\ \vdots \\ w(\mathbf{x} - \mathbf{x}^{(n)}) \mathbf{p}(\mathbf{x}^{(n)}) \end{array} \right\}^T \quad (31)$$

If the $\tilde{\mathbf{A}}$ matrix is non-singular and $n \geq m$ then

$$\mathbf{a}^{(i)}(\mathbf{x}) = \tilde{\mathbf{A}}^{-1}(\mathbf{x}, \mathbf{x}^{(j)}) \cdot \tilde{\mathbf{B}}(\mathbf{x}, \mathbf{x}^{(j)}) \cdot \hat{\mathbf{u}}^{(i)} \quad (32)$$

Taking Eqs.(26) and (32) someone obtains the MLS approximant of the displacement field

$$u_i(\mathbf{x}) = \mathbf{p}(\mathbf{x}) \cdot \tilde{\mathbf{A}}^{-1}(\mathbf{x}, \mathbf{x}^{(j)}) \cdot \tilde{\mathbf{B}}(\mathbf{x}, \mathbf{x}^{(j)}) \cdot \hat{\mathbf{u}}^{(i)} \quad (33)$$

Thus, it is easy for one to see that the MLS approximation of the displacement vector is

$$\mathbf{u}(\mathbf{x}) = \sum_{j=1}^n \phi_j(\mathbf{x}, \mathbf{x}^{(j)}) \hat{\mathbf{u}}(\mathbf{x}^{(j)}) \quad (34)$$

where $\hat{\mathbf{u}}(\mathbf{x}^{(j)})$ is the unknown fictitious displacement vector at node $\mathbf{x}^{(j)}$ and

$$\phi_j(\mathbf{x}, \mathbf{x}^{(j)}) = \sum_{l=1}^m p_l(\mathbf{x}) \left[\tilde{\mathbf{A}}^{-1}(\mathbf{x}, \mathbf{x}^{(j)}) \cdot \tilde{\mathbf{B}}(\mathbf{x}, \mathbf{x}^{(j)}) \right]_{lj} \quad (35)$$

Eq.(34) represents the MLS approximation of the displacement vector at the neighborhood of node \mathbf{x} .

Besides the displacement vectors, in the present work the traction vectors, defined at the points of the global boundary Γ , are considered as independent variables of the problem. Thus, their MLS approximation can be accomplished by means of the relation

$$\mathbf{t}(\mathbf{x}) = \sum_{j=1}^n \phi_j(\mathbf{x}, \mathbf{x}^{(j)}) \hat{\mathbf{t}}(\mathbf{x}^{(j)}) \quad (36)$$

where the fictitious nodal tractions $\hat{\mathbf{t}}(\mathbf{x}^{(j)})$ are zero for internal nodes and unknown vectors for the nodes lying on the boundary Γ . In other words, the approximation Eq.(36) utilizes all the nodal points belonging in the domain-of-definition of \mathbf{x} in order to define the shape functions $\phi_j(\mathbf{x}, \mathbf{x}^{(j)})$, it employs, however, only the traction vectors of the adjacent boundary nodes to approximate the traction vector at \mathbf{x} .

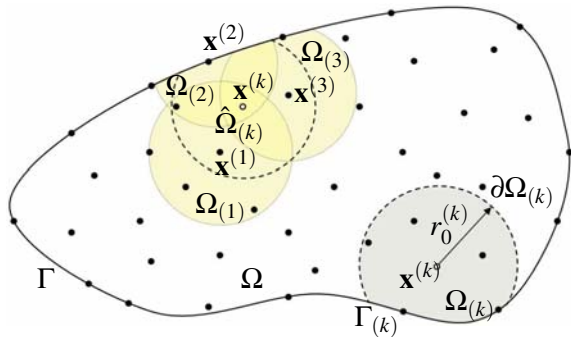


Figure 2 : The circular domain-of-influence $\Omega^{(k)}$ and the non-circular domain of definition $\hat{\Omega}^{(k)}$ used for the approximation of the field at $\mathbf{x}^{(k)}$.

4 Numerical implementation

In this section the numerical formulation of the proposed singular/hypersingular LBIE method is presented. Consider a set of N and M properly distributed points covering the internal domain Ω and the global boundary Γ , respectively, of the analyzed elastic body.

As it is mentioned in the previous section, the displacement LBIE (16) for an internal node $\mathbf{x}^{(k)}$ with a support domain $\Omega^{(k)}$ belonging entirely to Ω is (see Figs.1 and 2)

$$\mathbf{u}(\mathbf{x}^{(k)}) + \int_{\partial\Omega^{(k)}} \tilde{\mathbf{T}}^*(\mathbf{x}^{(k)}, \mathbf{y}) \cdot \mathbf{u}(\mathbf{y}) dS_{\mathbf{y}} + \int_{\Gamma^{(k)}} \tilde{\mathbf{T}}^*(\mathbf{x}^{(k)}, \mathbf{y}) \cdot \mathbf{u}(\mathbf{y}) dS_{\mathbf{y}} = \mathbf{0} \quad (37)$$

while for internal nodes the local domain of which intersects with the global boundary Γ , their LBIE (17) has the form

$$\mathbf{u}(\mathbf{x}^{(k)}) + \int_{\partial\Omega^{(k)}} \tilde{\mathbf{T}}^*(\mathbf{x}^{(k)}, \mathbf{y}) \cdot \mathbf{u}(\mathbf{y}) dS_{\mathbf{y}} + \int_{\Gamma^{(k)}} \tilde{\mathbf{T}}^*(\mathbf{x}^{(k)}, \mathbf{y}) \cdot \mathbf{u}(\mathbf{y}) dS_{\mathbf{y}} = \int_{\Gamma^{(k)}} \tilde{\mathbf{U}}^*(\mathbf{x}^{(k)}, \mathbf{y}) \cdot \mathbf{t}(\mathbf{y}) dS_{\mathbf{y}} \quad (38)$$

with the kernels $\tilde{\mathbf{U}}^*$, $\tilde{\mathbf{T}}^*$ representing $\tilde{\mathbf{U}}^* = \tilde{\mathbf{u}}^* - \tilde{\mathbf{u}}^c$ and $\tilde{\mathbf{T}}^* = \tilde{\mathbf{t}}^* - \tilde{\mathbf{t}}^c$.

Expanding both \mathbf{u} and \mathbf{t} according to the MLS approximation scheme of Eqs.(34) and (36), Eqs.(37) and (38) obtain the form

$$\sum_{j=1}^n \phi_j(\mathbf{x}^{(k)}, \mathbf{x}^{(j)}) \hat{\mathbf{u}}(\mathbf{x}^{(j)}) + \sum_{j=1}^n \tilde{\mathbf{H}}^{(k,j)} \cdot \hat{\mathbf{u}}(\mathbf{x}^{(j)}) = \mathbf{0} \quad (39)$$

$$\sum_{j=1}^n \phi_j(\mathbf{x}^{(k)}, \mathbf{x}^{(j)}) \hat{\mathbf{u}}(\mathbf{x}^{(j)}) + \sum_{j=1}^n [\tilde{\mathbf{H}}^{(k,j)} + \tilde{\mathbf{F}}^{(k,j)}] \cdot \hat{\mathbf{u}}(\mathbf{x}^{(j)}) = \sum_{j=1}^n \tilde{\mathbf{G}}^{(k,j)} \cdot \hat{\mathbf{t}}(\mathbf{x}^{(j)}) \quad (40)$$

where the tensors $\tilde{\mathbf{H}}^{(k,j)}$, $\tilde{\mathbf{F}}^{(k,j)}$, $\tilde{\mathbf{G}}^{(k,j)}$ correspond to integrals

$$\tilde{\mathbf{H}}^{(k,j)} = \int_{\partial\Omega^{(k)}} \tilde{\mathbf{T}}^*(\mathbf{x}^{(k)}, \mathbf{y}) \phi_j(\mathbf{y}, \mathbf{x}^{(j)}) dS_{\mathbf{y}} \quad (41)$$

$$\tilde{\mathbf{F}}^{(k,j)} = \int_{\Gamma^{(k)}} \tilde{\mathbf{T}}^*(\mathbf{x}^{(k)}, \mathbf{y}) \phi_j(\mathbf{y}, \mathbf{x}^{(j)}) dS_{\mathbf{y}} \quad (42)$$

$$\tilde{\mathbf{G}}^{(k,j)} = \int_{\Gamma^{(k)}} \tilde{\mathbf{U}}^*(\mathbf{x}^{(k)}, \mathbf{y}) \phi_j(\mathbf{y}, \mathbf{x}^{(j)}) dS_{\mathbf{y}} \quad (43)$$

For the k -th boundary node, both displacement and traction LBIEs, given by Eq.(17) and (25), respectively, are employed in the present formulation. More precisely, after the expansion of \mathbf{u} and \mathbf{t} according to the MLS ap-

proximation, Eqs.(17) and (25) are written as follows

$$\begin{aligned} & \frac{1}{2} \left[\tilde{\boldsymbol{\varepsilon}}_{\mathbf{u}} \cdot \mathbf{u} \left(\mathbf{x}^{(k)} \right) + \right. \\ & \left. \left(\tilde{\mathbf{I}} - \tilde{\boldsymbol{\varepsilon}}_{\mathbf{u}} \right) \cdot \sum_{j=1}^n \phi_j \left(\mathbf{x}^{(k)}, \mathbf{x}^{(j)} \right) \hat{\mathbf{u}} \left(\mathbf{x}^{(j)} \right) \right] + \\ & \sum_{j=1}^n \left[\tilde{\mathbf{H}}^{(k,j)} + \tilde{\mathbf{F}}^{(k,j)} \right] \cdot \hat{\mathbf{u}} \left(\mathbf{x}^{(j)} \right) = \\ & \sum_{j=1}^n \tilde{\mathbf{G}}^{(k,j)} \cdot \hat{\mathbf{t}} \left(\mathbf{x}^{(j)} \right) \end{aligned} \quad (44)$$

and

$$\begin{aligned} & \frac{1}{2} \left[\tilde{\boldsymbol{\varepsilon}}_{\mathbf{t}} \cdot \mathbf{t} \left(\mathbf{x}^{(k)} \right) + \right. \\ & \left. \left(\tilde{\mathbf{I}} - \tilde{\boldsymbol{\varepsilon}}_{\mathbf{t}} \right) \cdot \sum_{j=1}^n \phi_j \left(\mathbf{x}^{(k)}, \mathbf{x}^{(j)} \right) \hat{\mathbf{t}} \left(\mathbf{x}^{(j)} \right) \right] + \\ & \sum_{j=1}^n \left[\tilde{\mathbf{K}}^{(k,j)} + \tilde{\mathbf{E}}^{(k,j)} + \tilde{\mathbf{B}}^{(k,j)} \right] \cdot \hat{\mathbf{t}} \left(\mathbf{x}^{(j)} \right) = \\ & \sum_{j=1}^n \tilde{\mathbf{D}}^{(k,j)} \cdot \hat{\mathbf{t}} \left(\mathbf{x}^{(j)} \right) \end{aligned} \quad (45)$$

where the tensors $\tilde{\mathbf{K}}^{(k,j)}$, $\tilde{\mathbf{E}}^{(k,j)}$, $\tilde{\mathbf{D}}^{(k,j)}$, $\tilde{\mathbf{B}}^{(k,j)}$ correspond to integrals

$$\tilde{\mathbf{K}}^{(k,j)} = \int_{\partial\Omega^{(k)}} \tilde{\mathbf{P}}^* \left(\mathbf{x}^{(k)}, \mathbf{y} \right) \phi_j \left(\mathbf{y}, \mathbf{x}^{(j)} \right) dS_{\mathbf{y}} \quad (46)$$

$$\tilde{\mathbf{E}}^{(k,j)} = \int_{\Gamma^{(k)}} \tilde{\mathbf{P}}^* \left(\mathbf{x}^{(k)}, \mathbf{y} \right) \phi_j \left(\mathbf{y}, \mathbf{x}^{(j)} \right) dS_{\mathbf{y}} \quad (47)$$

$$\tilde{\mathbf{D}}^{(k,j)} = \int_{\Gamma^{(k)}} \tilde{\mathbf{V}}^* \left(\mathbf{x}^{(k)}, \mathbf{y} \right) \phi_j \left(\mathbf{y}, \mathbf{x}^{(j)} \right) dS_{\mathbf{y}} \quad (48)$$

$$\tilde{\mathbf{B}}^{(k,j)} = \int_{\Omega^{(k)}} \tilde{\mathbf{b}}^{\text{aux}} \left(\mathbf{x}^{(k)}, \mathbf{y} \right) \phi_j \left(\mathbf{y}, \mathbf{x}^{(j)} \right) dV_{\mathbf{y}} \quad (49)$$

with $\tilde{\mathbf{V}}^* = \tilde{\mathbf{v}}^* - \tilde{\mathbf{v}}^{\text{aux}}$, $\tilde{\mathbf{P}}^* = \tilde{\mathbf{p}}^* - \tilde{\mathbf{p}}^{\text{aux}}$ and

$$\tilde{\boldsymbol{\varepsilon}}_{\mathbf{u}, \mathbf{t}} = \begin{bmatrix} \boldsymbol{\varepsilon}_1^{u,t} & 0 \\ 0 & \boldsymbol{\varepsilon}_2^{u,t} \end{bmatrix} \quad (50)$$

The Greek indicators $\boldsymbol{\varepsilon}_1^{u,t}$, $\boldsymbol{\varepsilon}_2^{u,t}$ are equal to one for prescribed displacement or traction components and equal to zero when displacement or traction components are unknown on Γ .

For all N internal nodes, Eq.(39) and Eq.(40) are collocated while for the M boundary nodes Eq.(44) and Eq.(45) are employed. Thus, a system of linear algebraic equations is formed, i.e.

$$\begin{aligned} \tilde{\mathbf{W}}_I \cdot \hat{\mathbf{u}} + \tilde{\mathbf{Q}}_I \cdot \hat{\mathbf{t}} &= \mathbf{0}, \quad \text{for internal nodes} \\ \tilde{\mathbf{W}}_B \cdot \hat{\mathbf{u}} + \tilde{\mathbf{Q}}_B \cdot \hat{\mathbf{t}} &= \mathbf{f}, \quad \text{for boundary nodes} \end{aligned} \quad (51)$$

where $\hat{\mathbf{u}}$ and $\hat{\mathbf{t}}$ vectors denote the fictitious nodal displacement and traction vectors, respectively, while the vector \mathbf{f} contains the free displacement and traction terms of Eqs.(44) and (45), respectively, which correspond to the prescribed displacements and tractions on the global boundary Γ . The matrix $\tilde{\mathbf{W}}_I$ contains the $\tilde{\mathbf{H}}^{(k,j)}$, $\tilde{\mathbf{F}}^{(k,j)}$ tensors and the MLS interpolation functions of the displacements appearing in Eqs.(39) and (40). The matrix $\tilde{\mathbf{Q}}_I$ contains only the $\tilde{\mathbf{G}}^{(k,j)}$ tensor, while the matrix $\tilde{\mathbf{W}}_B$ contains the tensors: $\tilde{\mathbf{H}}^{(k,j)}$, $\tilde{\mathbf{F}}^{(k,j)}$, $\tilde{\mathbf{K}}^{(k,j)}$, $\tilde{\mathbf{E}}^{(k,j)}$, $\tilde{\mathbf{B}}^{(k,j)}$ and the MLS interpolation functions of the unknown displacements in Eq.(44). Finally, the matrix $\tilde{\mathbf{Q}}_B$ contains the $\tilde{\mathbf{G}}^{(k,j)}$, $\tilde{\mathbf{D}}^{(k,j)}$ tensors and the MLS interpolation functions of the unknown tractions in Eqs.(45).

In view of Eqs.(51), the following final system is obtained

$$\tilde{\mathbf{A}} \cdot \mathbf{z} = \mathbf{b} \quad (52)$$

with the vector \mathbf{z} comprising all the unknown fictitious displacements and tractions, while the vector \mathbf{b} contains the components of the prescribed vector \mathbf{f} .

This system can be solved numerically through a typical LU decomposition solver. As soon as, all the nodal fictitious displacements and tractions are calculated, the corresponding nodal values are retrieved through Eqs.(34), (36).

The integrals $\tilde{\mathbf{H}}^{(k,j)}$ and $\tilde{\mathbf{K}}^{(k,j)}$ are always regular since the collocation point $\mathbf{x}^{(k)}$ never gets close to the source point $\mathbf{y} \in \partial\Omega^{(k)}$. Similarly, volume integrals $\tilde{\mathbf{B}}^{(k,j)}$ are regular due to the regular nature of the kernel $\tilde{\mathbf{b}}^{\text{aux}}$. On the contrary, integrals $\tilde{\mathbf{G}}^{(k,j)}$ are weakly singular, $\tilde{\mathbf{F}}^{(k,j)}$ and $\tilde{\mathbf{D}}^{(k,j)}$ are strongly singular in the sense of Cauchy Principal Value, while integrals $\tilde{\mathbf{E}}^{(k,j)}$ appear a hypersingular behaviour. In the present work all the strongly singular and hypersingular integrals are evaluated with high accuracy by means of the advanced direct integration techniques proposed by [Guiggiani and Casalini (1987); Guiggiani, Krishnasamy, Rudolphi, and Rizzo (1992); Guiggiani (1994)]. Details on the evaluation of regular, singular, hypersingular and volume integrals can be found in the recent work of [Sellountos and Polyzos (2003)].

As soon as the fictitious displacements $\hat{\mathbf{u}}$ and the fictitious traction $\hat{\mathbf{t}}$ vectors defined at the global boundary Γ are evaluated, the MLS expansion schemes of Eqs.(34) and (36) are employed for the determination of the real displacement and traction vectors.

5 Examples

In this section, the accuracy of the proposed here Singular/Hypersingular LBIE method is demonstrated with the solution of two representative static elastic problems.

The first problem deals with a cylinder, of inner and outer radius $a = 1.2$ and $b = 2.0$, respectively, subjected to a uniform internal pressure $p_i = 100$. The material properties are taken $E = 10^3$ for Young modulus and $\nu = 0.25$ for Poisson ratio. Because of the symmetry only a quarter part of the cylinder is analyzed. In order to have a comparison with the MLPG (LBIE) method proposed recently by [Sellountos and Polyzos (2003)], the model is treated with 353 points, uniformly distributed along the boundary and inside to the body (Fig.3). The radii of the support domains is taken to be the same for all points and equal to 0.14177. The analytical radial displacements and stresses of this problem, expressed in polar coordinates (r, θ) , is given by [Timoshenko and Goodier (1970)]

$$u_r = p_i \frac{a^2 b^2}{b^2 - a^2} \frac{1 + \nu}{E} \left[\frac{1}{r} + \frac{(1 - 2\nu)r}{b^2} \right] \quad (53)$$

$$\sigma_{rr} = p_i \frac{a^2 b^2}{b^2 - a^2} \left(\frac{1}{b^2} - \frac{1}{r^2} \right) \quad (54)$$

The radial displacement and the corresponding traction field on the side $\theta = 0^\circ$ of the quarter part of the cylinder are numerically evaluated with both the MLPG (LBIE) method proposed by [Sellountos and Polyzos (2003)] and the singular/hypersingular MLPG (LBIE) technique demonstrated in the present paper. The obtained results are depicted in Figs.4 and 5. As it is evident, the agreement with the analytical solution is very good for both the MLPG (LBIE) methodologies, except for a small region near to the corner. This is due to the fact that there is no point exactly on the corner but two nodes from both sides and close each other. Thus, at these two points problems related to nearly singularities are observed.

The second problem concerns a 10×10 plate with a circular hole of radius $a = 1$ at the center, subjected to a uniform tensile load $p = 10$. The material properties are assumed to be $E = 2.4 \times 10^3$ and $\nu = 0.25$. Due to the symmetry, only the upper right quadrant of the plate is analyzed. For the solution of this problem 92 non-uniformly distributed points are considered (Fig.6). The support domain of each point is taken in such a way so as a well-defined integration star to be ensured [Liszka, Duarte, and Tworzydło (1996)]. The exact solutions for

displacement and stresses in polar coordinates are [Timoshenko and Goodier (1970)]

$$u_x = P \frac{1 + \nu}{E} \left[(1 - \nu)r \cos \theta + \frac{a^2}{2r} \cos 3\theta + 2(1 - \nu) \frac{a^2}{r} \cos \theta - \frac{a^4}{2r^3} \cos 3\theta \right] \quad (55)$$

$$u_y = P \frac{1 + \nu}{E} \left[-\nu r \sin \theta + \frac{a^2}{2r} \sin 3\theta - (1 - 2\nu) \frac{a^2}{r} \sin \theta - \frac{a^4}{2r^3} \sin 3\theta \right] \quad (56)$$

$$\sigma_{xx} = P \left[1 + \frac{3a^4}{2r^4} \cos 4\theta - \frac{a^2}{r^2} \left(\frac{3}{2} \cos 2\theta + \cos 4\theta \right) \right] \quad (57)$$

$$\tau_{xy} = P \left[\frac{3a^4}{2r^4} \sin 4\theta - \frac{a^2}{r^2} \left(\frac{1}{2} \sin 2\theta + \sin 4\theta \right) \right] \quad (58)$$

$$\sigma_{yy} = P \left[\frac{a^2}{r^2} \left(\cos 4\theta - \frac{1}{2} \cos 2\theta \right) - \frac{3a^4}{2r^4} \cos 4\theta \right] \quad (59)$$

The radial displacement u_r at $\theta = 45^\circ$ and the normal traction t_x for $\theta = 90^\circ$ are calculated and depicted in Figs.7 and 8, respectively. The obtained results are compared to the corresponding ones as well as to those taken by the MLPG (LBIE) method of [Sellountos and Polyzos (2003)]. It is observed that, except the corners, the agreement between the numerical and analytical results is very good, with the results of the singular/hypersingular MLPG (LBIE) method being better than those provided by the MLPG (LBIE) methodology of [Sellountos and Polyzos (2003)].

6 Conclusions

A new singular/hypersingular MLPG (LBIE) method for solving two dimensional problems has been proposed. It employs the displacement local boundary integral equation for the internal points, while for the boundary ones utilizes both the displacement and the corresponding traction local boundary integral equations. Thus, the essential displacement and traction boundary conditions of the problem are imposed by means of the free terms of the singular and hypersingular local boundary equations, respectively. This means that, for any distribution of nodal points, displacement and tractions can be treated as independent variables, avoiding thus calculating the derivatives of the MLS shape functions for the approxi-

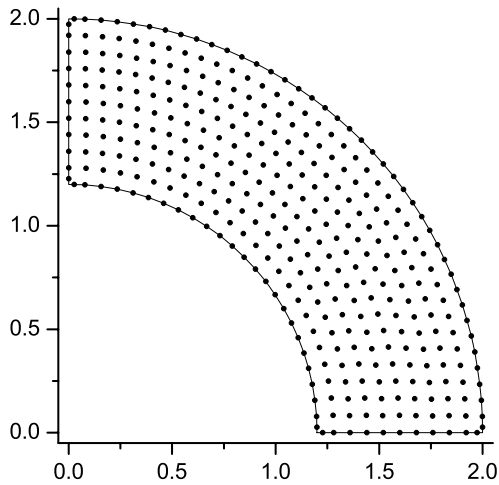


Figure 3 : Quarter cylinder being discretized with a uniform distribution of 353 nodes.

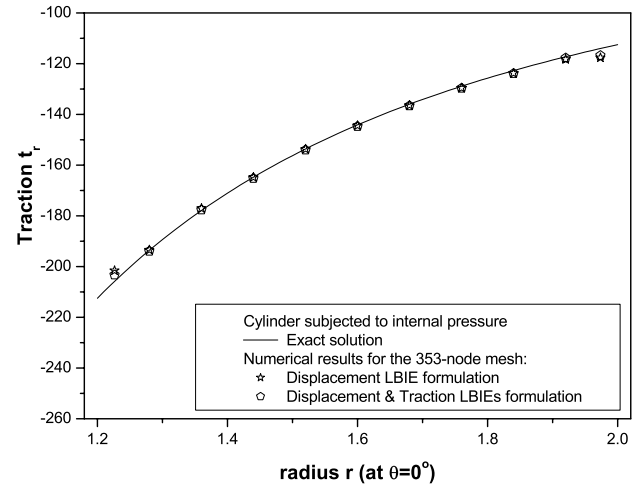


Figure 5 : Analytical versus numerical results of tractions for a 353 node distribution in the quarter cylinder at $y = 0$ and at $\theta = 0$.

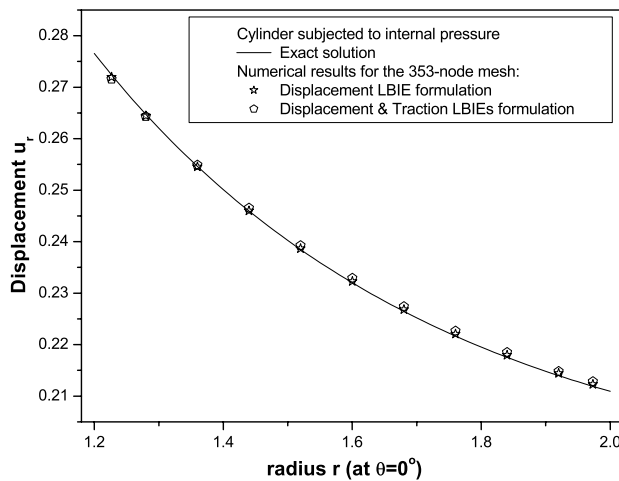


Figure 4 : Analytical versus numerical results of displacements for a 353 node distribution in the quarter cylinder at $y = 0$ and at $\theta = 0$.

mation of traction vectors.

Comparing the MLPG (LBIE) method of [Sellountos and Polyzos (2003)] with the present singular/hypersingular MLPG (LBIE) method, one can say that both methodologies provide accurate results for a uniform distribution of nodal points, while for non-uniform distributions the proposed here singular/hypersingular MLPG (LBIE) methodology is in general more accurate.

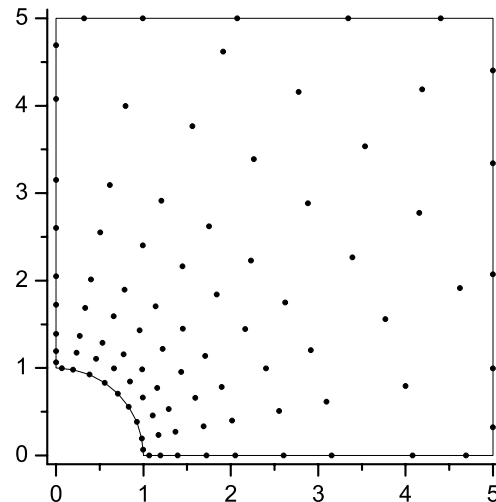


Figure 6 : Geometry and node distribution of the 92-node model of the plate with a hole.

Acknowledgement: The authors would like to thank the Greek Secretariat of Research and Technology and ENVIROCOUSTICS SA for the support at this work, in the framework of the PENED-2001 research program.

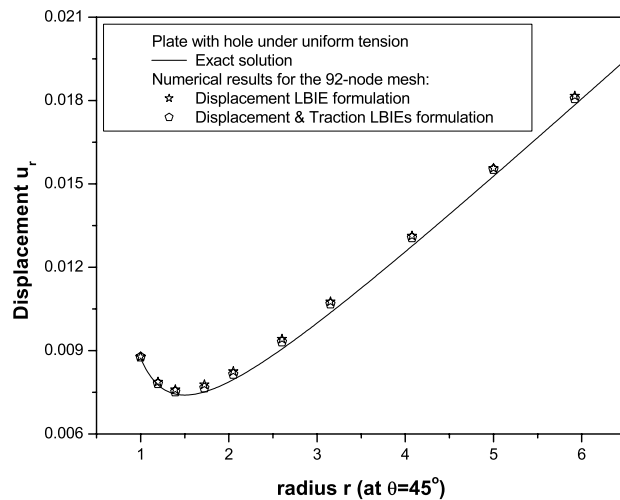


Figure 7 : Analytical versus numerical results of displacements for the 92-node distribution in the plate with a circular hole at $\theta = \pi/4$

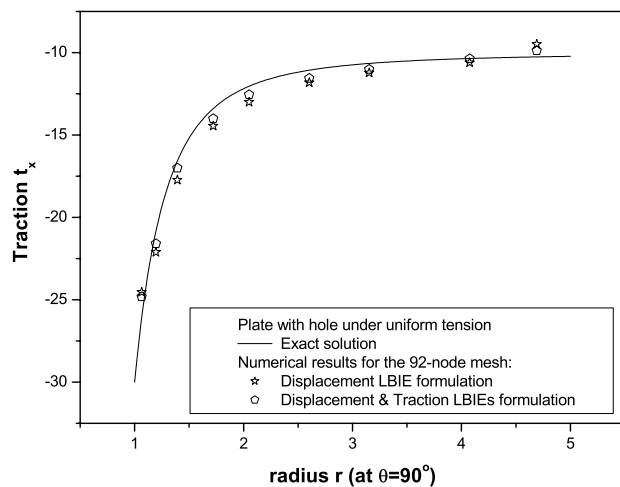


Figure 8 : Analytical versus numerical results of tractions for the 92-node distribution in the plate with a circular hole at $\theta = \pi/2$

References

Agnatiaris, J. P.; Polyzos, D. (2003): A boundary element method for acoustic scattering from non-axisymmetric and axisymmetric elastic shells. *CMES: Computer Modeling in Engineering & Sciences*, vol. 4,

pp. 197–212.

Atluri, S. N. (2004): *The Meshless Method (MLPG) for Domain & BIE Discretization*. Tech. Science Press.

Atluri, S. N.; Han, Z. D.; Shen, S. (2003): Meshless local Petrov-Galerkin (MLPG) approaches for solving the weakly-singular traction and displacement boundary integral equations. *CMES: Computer Modeling in Engineering & Sciences*, vol. 4, pp. 507–517.

Atluri, S. N.; Kim, H.-G.; Cho, J. Y. (1999): A critical assessment of the truly Meshless Local Petrov-Galerkin (MLPG) and Local Boundary Integral Equation (LBIE) methods. *Comput. Mech.*, vol. 24, pp. 348–372.

Atluri, S. N.; Shen, S. (2002a): *The Meshless Local Petrov-Galerkin (MLPG) Method*. Tech. Science Press.

Atluri, S. N.; Shen, S. (2002b): The meshless local Petrov-Galerkin (MLPG) method: A simple & less-costly alternative to the finite and boundary element method. *CMES: Computer Modeling in Engineering & Sciences*, vol. 3, pp. 11–52.

Atluri, S. N.; Sladek, J.; Sladek, V.; Zhu, T. (2000): The local boundary integral equation (LBIE) and its meshless implementation for linear elasticity. *Comput. Mech.*, vol. 25, pp. 180–198.

Atluri, S. N.; Zhu, T. (1998): A new meshless local Petrov-Galerkin (MLPG) approach in computation mechanics. *Comput. Mech.*, vol. 22, pp. 117–127.

Atluri, S. N.; Zhu, T. (2000): New concepts in meshless methods. *Int. J. Numer. Meth. Engrg.*, vol. 47, pp. 537–556.

Beskos, D. E. (1987): Boundary element methods in dynamic analysis. *Appl. Mech. Rev.*, vol. 40, pp. 1–23.

Beskos, D. E. (1997): Boundary element methods in dynamic analysis. Part II. *Appl. Mech. Rev.*, vol. 50, pp. 149–197.

Brebbia, C. A.; Dominguez, J. (1989): *Boundary Elements: An introductory course*. Computational Mechanics Publications, Southampton.

do Rego Silva, J. J. (1994): *Acoustic and Elastic Wave Scattering using Boundary Elements*. Computational Mechanics Publications, Southampton.

Gosz, S.; Liu, W. K. (1996): Admissible approximations for essential boundary conditions in the reproducing kernel particle method. *Comp. Mech.*, vol. 19, pp. 120–135.

- Guiggiani, M.** (1994): Hypersingular formulation for boundary stress evaluation. *Engrg. Anal. Boundary Elem.*, vol. 13, pp. 169–179.
- Guiggiani, M.; Casalini, P.** (1987): Direct computation of Cauchy principal value integrals in advanced boundary elements. *Int. J. Numer. Methods Engrg.*, vol. 24, pp. 1711–1720.
- Guiggiani, M.; Krishnasamy, G.; Rudolphi, T. J.; Rizzo, F. J.** (1992): A General Algorithm for the Numerical Solution of Hypersingular Boundary Integral Equations. *ASME J. Appl. Mechanics*, vol. 59, pp. 604–614.
- Han, Z. D.; Atluri, S. N.** (2004): Meshless local Petrov-Galerkin (MLPG) approaches for solving 3D Problems in elasto-statics. *CMES: Computer Modelling in Engineering & Sciences*, vol. 6, pp. 169–188.
- Krysl, P.; Belytschko, T.** (1997): Element-free Galerkin method: Convergence of the continuous and discontinuous shape functions. *Comp. Methods Appl. Mech. Engrg.*, vol. 148, pp. 257–277.
- Lancaster, P.; Salkauskas, K.** (1981): Surface generation by moving least square methods. *Math. Comput.*, vol. 37, pp. 141–158.
- Liszka, T. J.; Duarte, C. A. M.; Tworzydło, W. W.** (1996): hp-Meshless cloud method. *Comp. Methods Appl. Mech. Engrg.*, vol. 139, pp. 263–288.
- Long, S.; Zhang, Q.** (2002): Analysis of thin plates by the local boundary integral equation (LBIE) method. *Engrg. Anal. Boundary Elem.*, vol. 26, pp. 707–718.
- Polyzos, D.; Tsinopoulos, S. V.; Beskos, D. E.** (1998): Static and dynamic boundary element analysis in incompressible linear elasticity. *Eur. J. Mech., A/solids*, vol. 17, pp. 515–536.
- Qian, Z. Y.; Han, Z. D.; Atluri, S. N.** (2004): Directly Derived Non-Hyper-Singular Boundary Integral Equations for Acoustic Problems, and their Solution through Petrov-Galerkin Schemes. *CMES: Computer Modelling in Engineering & Sciences*, vol. 5, no. 6, pp. 541–562.
- Sellountos, E. J.; Polyzos, D.** (2003): A MLPG (LBIE) method for solving frequency domain elastic problems. *CMES: Computer Modelling in Engineering & Sciences*, vol. 4, pp. 619–636.
- Sellountos, E. J.; Polyzos, D.** (2004a): A meshless local boundary integral equation method for solving transient elastodynamic problems. *Comput. Mech.*
- Sellountos, E. J.; Polyzos, D.** (2004b): A MLPG (LBIE) approach in combination with BEM. *Comp. Methods Appl. Mech. Engrg.*
- Sladek, J.; Sladek, V.** (2003): Application of local boundary integral method in to micropolar elasticity. *Engrg. Anal. Boundary Elem.*, vol. 27, pp. 81–90.
- Sladek, J.; Sladek, V.; Atluri, S. N.** (2000a): Local boundary integral equation (LBIE) method for solving problems of elasticity with non-homogeneous material properties. *Comp. Mech.*, vol. 24, pp. 456–462.
- Sladek, J.; Sladek, V.; Atluri, S. N.** (2001): A pure contour formulation for meshless local boundary integral equation method in thermoelasticity. *CMES: Computer Modeling in Engineering & Sciences*, vol. 2, pp. 423–434.
- Sladek, J.; Sladek, V.; Atluri, S. N.** (2002): Application of the local boundary integral equation method to boundary value problems. *Int. J. Appl. Mech.*, vol. 38, pp. 1025–1043.
- Sladek, J.; Sladek, V.; Bazant, Z. P.** (2003): Non-local boundary integral formulation for softening damage. *Int. J. Numer. Meth. Engrg.*, vol. 57, pp. 103–116.
- Sladek, J.; Sladek, V.; Keer, R. V.** (2000): Numerical integration of singularities of local boundary integral equations. *Comp. Mech.*, vol. 25, pp. 394–403.
- Sladek, J.; Sladek, V.; Krivacek, J.; Zhang, C.** (2003): Local BIEM for transient heat conduction analysis in 3D axisymmetric functionally graded solids. *Comput. Mech.*, vol. 32, pp. 169–176.
- Sladek, J.; Sladek, V.; Mang, H. A.** (2002a): Meshless formulation for simply supported and clamped plate problems. *Int. J. Numer. Meth. Engrg.*, vol. 55, pp. 359–375.
- Sladek, J.; Sladek, V.; Mang, H. A.** (2002b): Meshless local boundary integral equation method for plates resting on the elastic foundation. *Comp. Meth. Appl. Mech. Eng.*, vol. 191, pp. 5943–5959.
- Sladek, J.; Sladek, V.; Mang, H. A.** (2003): Meshless formulations for simply supported and clamped plates under dynamic load. *Computers and Structures*, vol. 81, pp. 1643–1651.
- Timoshenko, S. P.; Goodier, J. N.** (1970): *Theory of Elasticity*. McGraw-Hill 3rd Edition, New York.

Zhu, T.; Zhang, J. D.; Atluri, S. N. (1998a): A local boundary integral equation (LBIE) method in computational mechanics and a meshless discretization approach. *Comp. Mech.*, vol. 21, pp. 223–235.

Zhu, T.; Zhang, J. D.; Atluri, S. N. (1998b): A meshless local boundary integral equation (LBIE) method for solving non-linear problems. *Comp. Mech.*, vol. 22, pp. 174–186.

Zhu, T.; Zhang, J. D.; Atluri, S. N. (1999): A meshless numerical method based on the local boundary integral equation (LBIE) to solve linear and non-linear boundary value problems. *Engng. Anal. Boundary Elem.*, vol. 23, pp. 375–389.

Appendix A: Auxiliary Local Integral Equation

In this appendix the auxiliary local integral equation, used for the elimination of tractions of Eq.(18) on the local boundary $\partial\Omega_x$, is explicitly derived.

Consider the displacement tensor function

$$\tilde{\mathbf{u}}^{\text{aux}} = \frac{1}{2\pi\mu} (\Psi^{\text{aux}} \tilde{\mathbf{I}} - X^{\text{aux}} \hat{\mathbf{r}} \otimes \hat{\mathbf{r}}) \quad (60)$$

where Ψ^{aux} and X^{aux} are regular functions of r , i.e.

$$\begin{aligned} \Psi^{\text{aux}} &= \sum_n A_n r^n, \quad n \geq 2 \\ X^{\text{aux}} &= \sum_n B_n r^n, \quad n \geq 2 \end{aligned} \quad (61)$$

Applying Betti's reciprocal identity for the displacement vector \mathbf{u} and the tensor $\tilde{\mathbf{u}}^{\text{aux}}$ in the support domain Ω_x , one obtains

$$\begin{aligned} \int_{\Omega_x} [\tilde{\mathbf{u}}^{\text{aux}}(\mathbf{x}, \mathbf{y}) \cdot \mathcal{D}_y \mathbf{u}(\mathbf{y}) - \mathcal{D}_y \tilde{\mathbf{u}}^{\text{aux}}(\mathbf{x}, \mathbf{y}) \cdot \mathbf{u}(\mathbf{y})] dV_y = \\ \int_{\partial\Omega_x \cup \Gamma_x} [\tilde{\mathbf{u}}^{\text{aux}}(\mathbf{x}, \mathbf{y}) \cdot \mathbf{t}(\mathbf{y}) - \tilde{\mathbf{t}}^{\text{aux}}(\mathbf{x}, \mathbf{y}) \cdot \mathbf{u}(\mathbf{y})] dS_y \end{aligned} \quad (62)$$

where the differential operator \mathcal{D}_y is given by Eq.(9) and

$$\begin{aligned} \tilde{\mathbf{t}}^{\text{aux}} = -\frac{1}{2\pi} \left\{ \left(\frac{X^{\text{aux}}}{r} - \frac{d\Psi^{\text{aux}}}{dr} \right) (\hat{\mathbf{r}} \cdot \hat{\mathbf{n}}) \tilde{\mathbf{I}} + \right. \\ \left. \left(\frac{X^{\text{aux}}}{r} - \frac{d\Psi^{\text{aux}}}{dr} \right) \hat{\mathbf{n}} \otimes \hat{\mathbf{r}} - \right. \\ \left. \left[\frac{2\nu}{1-2\nu} \left(\frac{d\Psi^{\text{aux}}}{dr} - \frac{dX^{\text{aux}}}{dr} - \frac{2X^{\text{aux}}}{r} \right) - \frac{2X^{\text{aux}}}{r} \right] \hat{\mathbf{r}} \otimes \hat{\mathbf{n}} + \right. \\ \left. 2 \left(\frac{dX^{\text{aux}}}{dr} - \frac{2X^{\text{aux}}}{r} \right) (\hat{\mathbf{r}} \cdot \hat{\mathbf{n}}) \hat{\mathbf{r}} \otimes \hat{\mathbf{r}} \right\} \end{aligned} \quad (63)$$

Taking into account that

$$\mathcal{D}_y \mathbf{u}(\mathbf{y}) = \mathbf{0} \quad (64)$$

and

$$\mathcal{D}_y \tilde{\mathbf{u}}^{\text{aux}}(\mathbf{x}, \mathbf{y}) = \tilde{\mathbf{B}}^{\text{aux}}(\mathbf{x}, \mathbf{y}) \quad (65)$$

where

$$\tilde{\mathbf{B}}^{\text{aux}} = \frac{1}{2\pi} [Q^{\text{aux}} \tilde{\mathbf{I}} - R^{\text{aux}} \hat{\mathbf{r}} \otimes \hat{\mathbf{r}}] \quad (66)$$

with

$$\begin{aligned} Q^{\text{aux}} &= \frac{d^2\Psi^{\text{aux}}}{dr^2} + \frac{1}{r} \frac{d\Psi^{\text{aux}}}{dr} - \frac{2X^{\text{aux}}}{r^2} + \\ &\frac{1}{1-2\nu} \left(\frac{1}{r} \frac{d^2\Psi^{\text{aux}}}{dr^2} - \frac{1}{r} \frac{dX^{\text{aux}}}{dr} - \frac{X^{\text{aux}}}{r^2} \right) \\ R^{\text{aux}} &= -\frac{d^2X^{\text{aux}}}{dr^2} - \frac{1}{r} \frac{dX^{\text{aux}}}{dr} + \frac{4X^{\text{aux}}}{r^2} + \\ &\frac{1}{1-2\nu} \left(\frac{d^2\Psi^{\text{aux}}}{dr^2} - \frac{1}{r} \frac{d\Psi^{\text{aux}}}{dr} - \frac{d^2X^{\text{aux}}}{dr^2} + \frac{2X^{\text{aux}}}{r^2} \right) \end{aligned} \quad (67)$$

the integral Eq.(62) obtains the form

$$\begin{aligned} \int_{\partial\Omega_x \cup \Gamma_x} [\tilde{\mathbf{t}}^{\text{aux}}(\mathbf{x}, \mathbf{y}) \cdot \mathbf{u}(\mathbf{y}) - \tilde{\mathbf{u}}^{\text{aux}}(\mathbf{x}, \mathbf{y}) \cdot \mathbf{t}(\mathbf{y})] dS_y = \\ \int_{\Omega_x} \tilde{\mathbf{B}}^{\text{aux}}(\mathbf{x}, \mathbf{y}) \cdot \mathbf{u}(\mathbf{y}) dV_y \end{aligned} \quad (68)$$

The application of the operator $\hat{\mathbf{n}}_x \cdot \nabla_x$ on Eq.(68) yields

$$\begin{aligned} \int_{\partial\Omega_x \cup \Gamma_x} [\tilde{\mathbf{p}}^{\text{aux}}(\mathbf{x}, \mathbf{y}) \cdot \mathbf{u}(\mathbf{y}) - \tilde{\mathbf{v}}^{\text{aux}}(\mathbf{x}, \mathbf{y}) \cdot \mathbf{t}(\mathbf{y})] dS_y = \\ \int_{\Omega_x} \tilde{\mathbf{b}}^{\text{aux}}(\mathbf{x}, \mathbf{y}) \cdot \mathbf{u}(\mathbf{y}) dV_y \end{aligned} \quad (69)$$

where

$$\begin{aligned} \tilde{\mathbf{v}}^{\text{aux}}(\mathbf{x}, \mathbf{y}) = \frac{1}{2\pi} \left\{ \left(\frac{X^{\text{aux}}}{r} - \frac{d\Psi^{\text{aux}}}{dr} \right) [\hat{\mathbf{n}}_x \otimes \hat{\mathbf{r}} + (\hat{\mathbf{n}}_x \cdot \hat{\mathbf{r}}) \tilde{\mathbf{I}}] - \right. \\ \left. \left[\frac{2\nu}{1-2\nu} \left(\frac{d\Psi^{\text{aux}}}{dr} - \frac{dX^{\text{aux}}}{dr} - \frac{X^{\text{aux}}}{r} \right) - \frac{2X^{\text{aux}}}{r} \right] \hat{\mathbf{r}} \otimes \hat{\mathbf{n}}_x + \right. \\ \left. 2 \left(\frac{dX^{\text{aux}}}{dr} - \frac{2X^{\text{aux}}}{r} \right) (\hat{\mathbf{n}}_x \cdot \hat{\mathbf{r}}) \hat{\mathbf{r}} \otimes \hat{\mathbf{r}} \right\} \end{aligned} \quad (70)$$

$$\begin{aligned} \tilde{\mathbf{p}}^{\text{aux}}(\mathbf{x}, \mathbf{y}) = \frac{\mu}{2\pi} [\beta_1(r) (\hat{\mathbf{n}}_y \cdot \hat{\mathbf{r}}) \hat{\mathbf{n}}_x \otimes \hat{\mathbf{r}} + \\ \beta_2(r) (\hat{\mathbf{n}}_y \cdot \hat{\mathbf{r}}) (\hat{\mathbf{n}}_x \cdot \hat{\mathbf{r}}) \tilde{\mathbf{I}} + \beta_2(r) (\hat{\mathbf{n}}_y \cdot \hat{\mathbf{r}}) \hat{\mathbf{r}} \otimes \hat{\mathbf{n}}_x - \\ \beta_3(r) (\hat{\mathbf{n}}_y \cdot \hat{\mathbf{r}}) (\hat{\mathbf{n}}_x \cdot \hat{\mathbf{r}}) \hat{\mathbf{r}} \otimes \hat{\mathbf{r}} + \beta_2(r) (\hat{\mathbf{n}}_y \cdot \hat{\mathbf{n}}_x) \hat{\mathbf{r}} \otimes \hat{\mathbf{r}} + \\ \beta_2(r) (\hat{\mathbf{n}}_x \cdot \hat{\mathbf{r}}) \hat{\mathbf{n}}_y \otimes \hat{\mathbf{r}} + \beta_1(r) (\hat{\mathbf{n}}_x \cdot \hat{\mathbf{r}}) \hat{\mathbf{r}} \otimes \hat{\mathbf{n}}_y + \\ \beta_4(r) (\hat{\mathbf{n}}_y \cdot \hat{\mathbf{n}}_x) \tilde{\mathbf{I}} + \beta_4(r) \hat{\mathbf{n}}_y \otimes \hat{\mathbf{n}}_x - \beta_5(r) \hat{\mathbf{n}}_x \otimes \hat{\mathbf{n}}_y] \end{aligned} \quad (71)$$

with

$$\begin{aligned} \beta_1(r) &= 4 \left(\frac{1}{r} \frac{dX^{\text{aux}}}{dr} - \frac{2X^{\text{aux}}}{r} \right) + \\ &\frac{4\nu}{1-2\nu} \left(\frac{d^2X^{\text{aux}}}{dr^2} - \frac{d^2\Psi^{\text{aux}}}{dr^2} + \frac{1}{r} \frac{d\Psi^{\text{aux}}}{dr} - \frac{2X^{\text{aux}}}{r^2} \right) \\ \beta_2(r) &= -\frac{d^2\Psi^{\text{aux}}}{dr^2} + \frac{1}{r} \frac{d\Psi^{\text{aux}}}{dr} + \frac{3}{r} \frac{dX^{\text{aux}}}{dr} - \frac{6X^{\text{aux}}}{r^2} \\ \beta_3(r) &= -4 \left(\frac{d^2X^{\text{aux}}}{dr^2} - \frac{5}{r} \frac{dX^{\text{aux}}}{dr} + \frac{8X^{\text{aux}}}{r^2} \right) \\ \beta_4(r) &= 2 \left(\frac{X^{\text{aux}}}{r^2} - \frac{1}{r} \frac{d\Psi^{\text{aux}}}{dr} \right) \\ \beta_5(r) &= -\frac{4X^{\text{aux}}}{r^2} - \frac{8\nu}{1-2\nu} \left(\frac{1}{r} \frac{dX^{\text{aux}}}{dr} - \frac{1}{r} \frac{d\Psi^{\text{aux}}}{dr} + \frac{X^{\text{aux}}}{r^2} \right) + \\ &\left(\frac{2\nu}{1-2\nu} \right)^2 \left(\frac{d^2\Psi^{\text{aux}}}{dr^2} - \frac{d^2X^{\text{aux}}}{dr^2} - \frac{2}{r} \frac{dX^{\text{aux}}}{dr} + \frac{1}{r} \frac{d\Psi^{\text{aux}}}{dr} \right) \end{aligned} \quad (72)$$

and

$$\begin{aligned} \tilde{\mathbf{b}}^{\text{aux}}(\mathbf{x}, \mathbf{y}) = & \frac{dQ^{\text{aux}}}{dr} (\hat{\mathbf{n}}_{\mathbf{x}} \cdot \hat{\mathbf{r}}) \tilde{\mathbf{I}} + \frac{R^{\text{aux}}}{r} (\hat{\mathbf{r}} \otimes \hat{\mathbf{n}}_{\mathbf{x}} + \hat{\mathbf{n}}_{\mathbf{x}} \otimes \hat{\mathbf{r}}) + \\ & \left(\frac{dR^{\text{aux}}}{dr} - \frac{2R^{\text{aux}}}{r} \right) (\hat{\mathbf{n}}_{\mathbf{x}} \cdot \hat{\mathbf{r}}) \hat{\mathbf{r}} \otimes \hat{\mathbf{r}} \end{aligned} \quad (73)$$

On the local boundary $\partial\Omega_{\mathbf{x}}$, the tensor function $\tilde{\mathbf{v}}^{\text{aux}}$ is imposed to satisfy the condition

$$\tilde{\mathbf{v}}^{\text{aux}}(\mathbf{x}, \mathbf{y}) = \tilde{\mathbf{v}}^*(\mathbf{x}, \mathbf{y}), \quad \mathbf{y} \in \partial\Omega_{\mathbf{x}} \quad (74)$$

where $\tilde{\mathbf{v}}^*$ the kernel provided by Eq.(19).

In view of Eq.(19) and Eqs.(61), (70), it is easy to find one that Eq.(74) is satisfied when

$$\begin{aligned} A_2 &= -\frac{3}{4(1-\nu)} \frac{1}{r_0^2} \\ A_3 &= \frac{1}{2(1-\nu)} \frac{1}{r_0^3} \\ A_4 &= A_5 = \dots = 0 \\ B_2 &= -\frac{3-4\nu}{8(1-\nu)} \frac{1}{r_0^2} \\ B_3 &= B_4 = \dots = 0 \end{aligned} \quad (75)$$

Thus, the specific values of X^{aux} and Ψ^{aux} , i.e.

$$\begin{aligned} X^{\text{aux}} &= -\frac{3}{4(1-\nu)} \frac{r^2}{r_0^2} + \frac{1}{2(1-\nu)} \frac{r^3}{r_0^3} \\ \Psi^{\text{aux}} &= -\frac{3-4\nu}{8(1-\nu)} \frac{r^2}{r_0^2} \end{aligned} \quad (76)$$

in conjunction with Eq.(69), form the auxiliary local boundary equation used in section 2.2 for the elimination of tractions on the local boundary $\partial\Omega_{\mathbf{x}}$.

